TIME-SHARING MEASUREMENTS OF IONOSPHERIC ELECTRON TEMPERATURE AND ELECTRON DENSITY WITH THE ELECTRIC FIELD USING DOUBLE PROBES: AN EXPERIMENT ON THE ANTARCTIC SOUNDING ROCKET S-310JA-7

Toshio OGAWA, Masahiko MAKINO,

Geophysical Institute, Kyoto University, Kitashirakawa Oiwake-cho, Sakyo-ku, Kyoto 606

Hisao YAMAGISHI, Hiroshi FUKUNISHI, Takeo HIRASAWA

National Institute of Polar Research, 9–10, Kaga 1-chome, Itabashi-ku, Tokyo 173

and

Kunihiko KODERA

Meteorological Research Institute, 1–1, Nagamine, Yatabe-cho, Tsukuba-gun, Ibaraki 305

Abstract: An experiment was carried out of a time-sharing measurement of auroral ionospheric electric field, electron temperature and electron density with double probes on board the Antarctic sounding roket S-310JA-7 on March 27, 1978 at Syowa Station. The measurements of each element are compared with each other, and the electron temperature and density are compared with the other independent measurements which were made simultaneously on board the same rocket. The principle of the measurement of electron temperature and density with double probes is described in detail in the Appendix.

1. Introduction

Ionospheric electric field measurements with double probes have been made by several Antarctic sounding rockets during both disturbed and quiet periods at Syowa Station (OGAWA *et al.*, 1979, 1980, 1981). The double probe method is superior for the electric field measurement due to its characteristic feature of common mode error rejection. This method may also be applied to the measurement of electron temperature and electron density. For geophysical research, the electron temperature and the electron density are the fundamental elements of the ionospheric plasma and it would be very convenient if time-sharing measurements of these two elements with the electric field were made using the same double probes. The experimental basis of these measurements is described and an example is given which was obtained by the Antarctic sounding rocket S-310JA-7 on March 27, 1978 at Syowa Station. The results of the DC and AC electric field measurements are given separately by OGAWA *et al.* (1981) and YAMAGISHI *et al.* (1981) respectively. Details of the principle of the measurements are given in the Appendix.

2. Experimental Basis

Two pairs of double probes were mounted on the Antarctic sounding rocket S-310JA-7. Spherical probes 4 cm in diameter, gold-plated and aquadag-coated, were attached at the tips of each of two insulated booms deployed symmetrically in the horizontal plane. The distance between the probes was 2.45 m. Preamplifiers of a follower type were inserted within the hollow probes. Input resistances of $1\times 10^9\,\Omega$ and $1\times 10^6\,\Omega$ were used alternately by switching. A second pair of probes was placed at the tip of the rocket separated from the first by 47 cm along the rocket axis. By a time-sharing use of these probes measurements were planned of electron temperature and electron density as well as DC and AC electric fields.

The following is the experimental basis of measuring the electron temperature and the electron density with double probes assuming that the distribution of electron thermal velocities is Maxwellian. Probes 1 and 2 constitute a pair of double probes. The circuit diagram of the double probe preamplifier is given in Fig. 1, and representative Langmuir probe characteristic curves of the two probes are given in Fig. 2. The

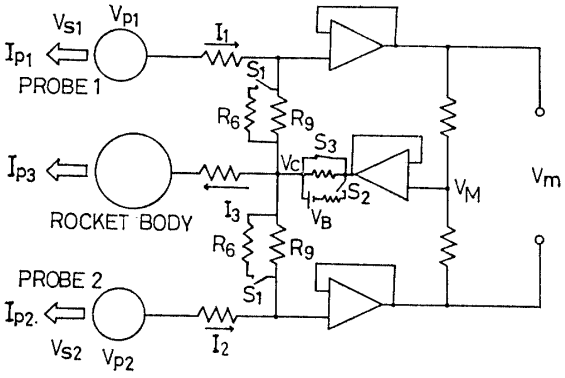

Fig. 1. Circuit diagram of the double probe preamplifier.

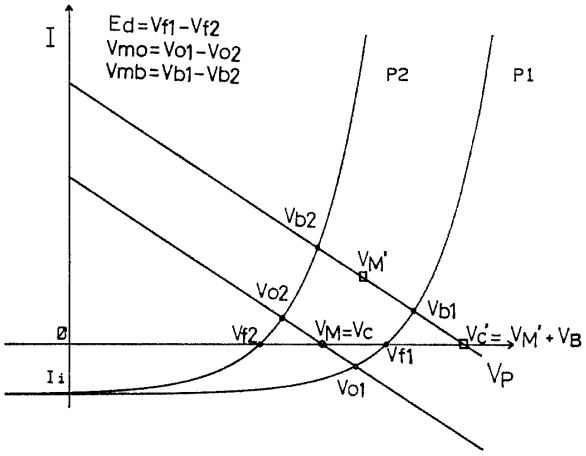

Fig. 2. Langmuir curves of the double probes.

electric field, the electron temperature and the electron density are measured by changing the input resistances of the differential preamplifier from $R_9(=10^9\,\Omega)$ to $R_6(=10^6\,\Omega)$ alternately by operating the two switches S_1 simultaneously. When the switches S_1 are open, that is when the input resistances are $10^9\Omega$, the two probes are supposed to be floating and the DC electric field will be measured. In Fig. 2, as the input current is zero at this time, the potentials of the probes 1 and 2 are at the floating potentials, V_{f1} and V_{f2}, respectively, and the applied voltage to the double probes, $Ed(=V_{f1}-V_{f2})$, is the ambient ionospheric electric field plus the induced field $v\times B$, where v is the velocity of the probes which are carried by the rocket and B the magnetic induction. When the switches S_1 are closed, that is when the input resistances are $10^6\Omega$, two measurement modes are selected by opening/closing the switch S_2 and closing/opening the switch S_3 simultaneously. In the first mode we only change the input resistances to $10^6\Omega$, and in the second mode in addition to this we apply the bias voltage

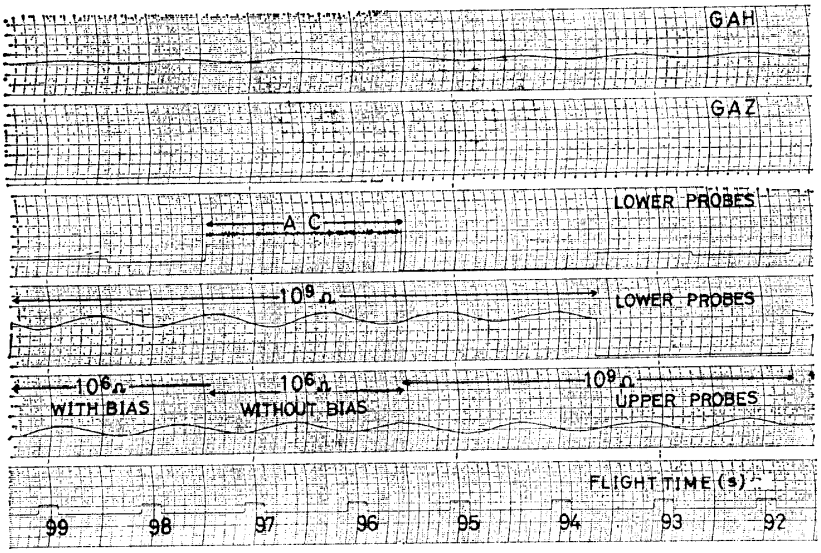

Fig. 3. An example of the record obtained.

V_B(=0.1 V) to the two probes. The output voltages with and without the bias are V_{mb} and V_{mo}, respectively. Figure 3 shows an example of the observed record. Ed is measured for a period of 4 s, V_{mo} for 2 s, and V_{mb} for 2 s during a total cycle of 8 s. From these three voltages Ed, V_{mo}, and V_{mb}, the electron temperature T_e and electron density N_e are calculated using the following equations;

$$T_e=\frac{eV_B}{k}\left(\frac{1}{Ed/V_{mb}-1}-\frac{1}{Ed/V_{mo}-1}\right)^{-1}, \tag{1}$$

$$N_e=\frac{1}{4\pi r^2}\frac{V_B}{eR_6}\left\{\frac{V_{mb}(Ed-V_{mo})}{V_{mo}(Ed-V_{mb})}-1\right\}^{-1}\left(\frac{kT_i}{2\pi m_i}+\frac{v_R^2}{16}\right)^{-1/2}, \tag{2}$$

where e is the absolute electronic charge, k is the Boltzmann's constant, r is the probe radius, T_i is the ion temperature, m_i is the ion mass, and v_R is the rocket velocity. When we estimate the electron density, we need to assume the ion temperature T_i, and the ion mass m_i. Details of the derivation of eqs. (1) and (2) are given in the Appendix.

3. Results and Discussions

The Antarctic sounding rocket S-310JA-7 was launched at 1915: 50 UT (2215: 50 EST) on March 27, 1978 from Syowa Station into an active auroral arc. The results of DC and AC electric field measurements are given by OGAWA *et al.* (1981) and YAMAGISHI *et al.* (1981), respectively. The electron temperature estimated from eq. (1) is plotted in Fig. 4. The circles show the temperature during the rocket ascent and the crosses show that during the rocket descent. The estimated errors are shown by the error bars. The electron temperature was 1000 K in the auroral arc at an altitude of about 105 km and decreased to 400 K out of the arc. The electron temperature then increased with altitude to 2000 K at an altitude of 220 km. It had a large variation in the altitude range of 180–200 km. The electron temperature during the descent was nearly the same as that during the ascent except in the altitude range

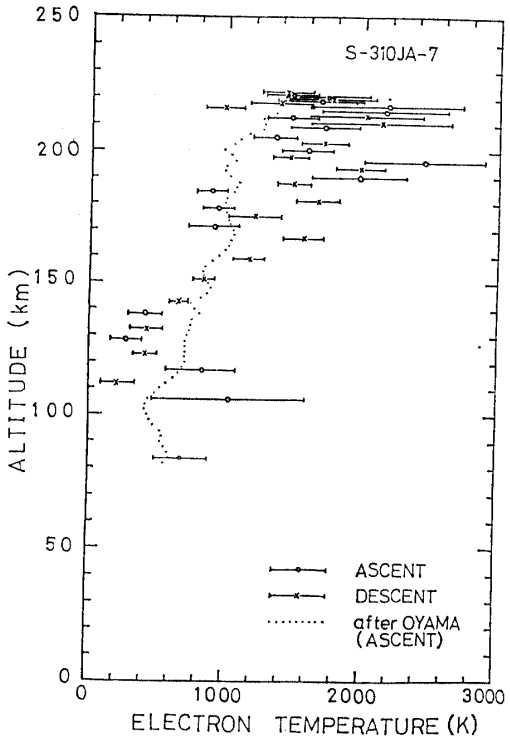

Fig. 4. Altitude profiles of the estimated electron temperature.

from 190 to 170 km where the descent values were larger than the ascent values.

On the same rocket flight, the electron temperature was measured with the standard electron temperature probe (OYAMA and HIRAO, 1981), which is given by the dotted line in Fig. 4. Although large differences between the present result and the OYAMA and HIRAO's result can be seen around the altitudes of 100 km and 190 km, the general trends of both temperatures are compatible with each other to within about ± 400 K. As the probes went through and near the auroral arcs at these altitudes (see OGAWA *et al.*, 1981), the assumed Maxwell's velocity distribution of the thermal electrons would not hold because of the precipitating auroral particles. According to the OYAMA's private communication, the presently obtained temperature profile is similar to the result estimated by the second harmonic method which will be described by himself elsewhere. OYAMA said that the estimated electron energy distribution shifted toward lower energies at an altitude of about 100 km and toward higher energies at about 190 km. In these conditions the definition of the temperature itself becomes obscure.

The electron density, which was estimated from eq. (2) is plotted in Fig. 5 with the assumption that the ion mass was 30 amu and the ion temperature T_i, was equal to the electron temperature T_e, and to half of it $T_e/2$. The circles show the density for $T_i=T_e$ and the squares show that for $T_i=T_e/2$. The white symbols show the density during the rocket ascent and the black symbols show that during the rocket descent. The difference between the two cases is larger at the higher altitudes than at the lower altitudes but the magnitude is not very large compared with the altitude variation. Neglecting small scale disturbances the electron density increased with altitude from 2×10^{11} m^{-3} to 9×10^{11} m^{-3}. The density during the descent was about 50% smaller than that during the ascent. In the auroral arc at an altitude of about

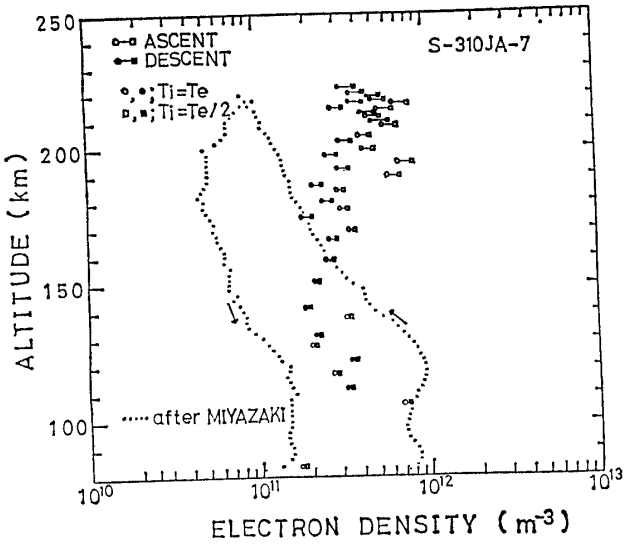

Fig. 5. Altitude profiles of the estimated electron density.

105 km and out of the auroral arc at an altitude of about 195 km in the ascent profile the electron density was about twice as large as the descent values. As suggested for the measured temperature profile, these enhancements of the electron density may also be due to a non-Maxwellian distribution of thermal electrons.

On the same rocket flight, the electron density was measured by the electron current flowing into the grid of the Faraday cup (MIYAZAKI *et al.*, 1981). The result of their measurements is given by the dotted line in Fig. 5. Their values are different by about an order of magnitude between the ascent and descent values. In contrast the profile of the electron density estimated from the double probe method does not much change between the ascent and the descent. The two profiles are essentially different and not suitable for comparison with each other.

In Fig. 6 the three sets of data are plotted together, the DC electric field $|\boldsymbol{E}|$, the electron density N_e, and the electron temperature T_e, all of which were measured by the same double probes. The DC electric field in Fig. 6 was estimated assuming no $\boldsymbol{B}$-parallel electric field. The data showing large variations of electric field in the altitude range of 110–80 km during the rocket descent are poor in quality; the spin modulated waveforms are distorted. Therefore, we do not pay much attention to this period of data.

Comparing the three profiles the following points are noted:

(1) The electric field is about twice as large during the rocket descent as during the ascent.

(2) The electron density is about 50% larger during the rocket ascent than during the descent.

(3) A weak anticorrelation is observed between the electric field and electron density profiles.

(4) It seems to the authors that the facts (1) to (3) will give the latitudinal distributions of these elements in respect to the appearance of aurora; the electric field is smaller in the auroral region than the equator side of it, and the electron density

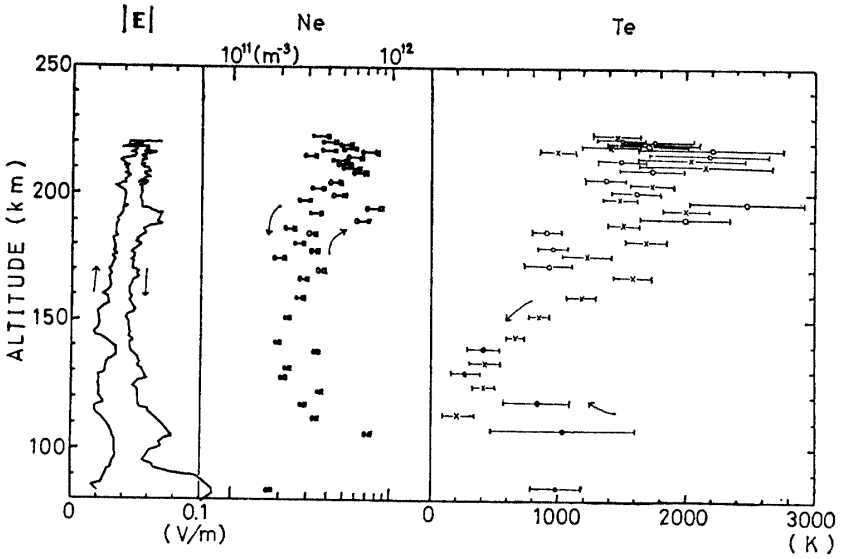

Fig. 6. Comparison of observed electric field, electron density and electron temperature estimated using the same double probes.

change is opposite to that of the electric field.

(5) Correlation between the electric field and the electron temperature is obscure.

As the auroral activity was extremely large during the period of this experiment, the plasma characteristics would be changing greatly in the ionosphere. This would make the present experimental results less clear. If the measurements had been made during a less active period, the double probe method of estimating the electron temperature and the electron density described in this paper might have given results more compatible with the electric field, although the time-sharing method can not give continuous data.

References

MIYAZAKI, S., OGAWA, T., MORI, H. and YAMAGISHI, H. (1981): Observational results of electron density profile by S-310JA-7 rocket. Mem. Natl Inst. Polar Res., Spec. Issue, **18**, 300–303.

OGAWA, T., IWAGAMI, N. and AYUKAWA, M. (1980): Nankyoku roketto S-210JA-29-goki ni yoru seion-ji kabu-denrisô denba no kansoku (Measurement of quiet-time electric field in the lower ionosphere by the Antarctic sounding rocket S-210JA-29). Nankyoku Shiryô (Antarct. Rec.), **68**, 88–96.

OGAWA, T., MORITA, M., FUKUNISHI, H., MATSUO, T. and YOSHINO, T. (1979): Nankyoku roketto S-210JA-24, 25-gôki ni yoru denrisô denba no kansoku (Measurements of ionospheric electric fields with Antarctic sounding rockets S-210JA-24 and 25). Nankyoku Shiryô (Antarct. Rec.), **63**, 252–275.

OGAWA, T., MAKINO, M., HAYASHIDA, S., YAMAGISHI, H., FUJII, R., FUKUNISHI, H., HIRASAWA, T. and NISHINO, M. (1981): Measurement of auroral electric fields with an Antarctic sounding rocket S-310JA-7. 1. DC electric field. Mem. Natl Inst. Polar Res., Spec. Issue, **18**, 355–378.

OYAMA, K.-I. and HIRAO, K. (1981): Gross features of electron temperature profile of polar ionosphere. Mem. Natl Inst. Polar Res., Spec. Issue, **18**, 330–334.

YAMAGISHI, H., FUKUNISHI, H., HIRASAWA, T. and OGAWA, T. (1981): Measurement of auroral elec-

tric fields with an Antarctic sounding rocket S-310JA-7. 2. AC electric field. Mem. Natl Inst. Polar Res., Spec. Issue, **18**, 379–390.

(Received December 24, 1981; Revised manuscript received February 1, 1982)

Appendix: Principle of the Measurements

The probe current I_p, which is a function of the probe potential V_p, is expressed as

$$I_p(V_p)=I_e(V_p)+I_i=I_e \exp\left\{\frac{e(V_p-V_s)}{kT_e}\right\}+I_i\,, \tag{A-1}$$

where $I_e(V_p)$ is the electron current, I_i is the ion current, V_s is the space potential, T_e is the electron temperature, e is the absolute electronic charge, and k is Boltzmann's constnat. Here, it is assumed that the electron thermal velocity distribution is Maxwellian and the ion current is independent of the probe potential. The probe current will be zero when the probes are floating, that is

$$I_p(V_f)=I_e(V_f)+I_i=0\,, \tag{A-2}$$

where V_f is the floating potential. Therefore,

$$I_i=-I_e \exp\left\{\frac{e(V_f-V_s)}{kT_e}\right\}\,. \tag{A-3}$$

The circuit current which flows through the input resistances is expressed as

$$I_c(V_p)=\frac{V_p-V_c}{R}\,, \tag{A-4}$$

where R is the input resistance, and V_c is the reference potential within the circuit in Fig. 1. The relation between the probe current I_p, and the circuit current I_c, is given by

$$I_p(V_p)-I_c(V_p)=0\,. \tag{A-5}$$

By substituting eq. (A-3) in eq. (A-1), we obtain the equation

$$\frac{I_p(V_p)}{I_i}=-\exp\left\{\frac{e(V_p-V_f)}{kT_e}\right\}+1\,. \tag{A-6}$$

By substituting eq. (A-4) in eq. (A-5) and by using eq. (A-6), we obtain the equation

$$\exp\left\{\frac{e(V_p-V_f)}{kT_e}\right\}-1+\frac{V_p-V_c}{RI_i}=0\,. \tag{A-7}$$

As eq. (A-7) can be applied for the double probes,

$$\exp\left\{\frac{e(V_{p1}-V_{f1})}{kT_e}\right\}-1+\frac{V_{p1}-V_c}{RI_i}=0\,, \tag{A-8}$$

$$\exp\left\{\frac{e(V_{p2}-V_{f2})}{kT_e}\right\}-1+\frac{V_{p2}-V_c}{RI_i}=0\,, \tag{A-9}$$

where suffixes 1 and 2 express the probes 1 and 2, respectively. The measured voltage V_m at the output circuit and the applied voltage Ed when floating are expressed respectively by

$$V_m = V_{p1} - V_{p2}\,, \tag{A-10}$$

$$Ed = V_{f1} - V_{f2}\,. \tag{A-11}$$

Using eqs. (A-10) and (A-11), we express the potentials V_{p1}, V_{p2}, V_{f1} and V_{f2} as

$$\left.\begin{aligned} V_{p1} &= \bar{V}_p + V_m/2\,, \\ V_{p2} &= \bar{V}_p - V_m/2\,, \\ V_{f1} &= \bar{V}_f + Ed/2\,, \\ V_{f2} &= \bar{V}_f + Ed/2\,, \end{aligned}\right\} \tag{A-12}$$

where

$$\left.\begin{aligned} \bar{V}_p &= (V_{p1} + V_{p2})/2\,, \\ \bar{V}_f &= (V_{f1} + V_{f2})/2\,. \end{aligned}\right\} \tag{A-13}$$

By substituting eq. (A-12) in eq. (A-8) and eq. (A-9), we obtain two equations

$$\exp\left\{\frac{e(\bar{V}_p - \bar{V}_f)}{kT_e}\right\} \exp\left\{\frac{e(V_m - Ed)}{2kT_e}\right\} - 1 + \frac{\bar{V}_p + V_m/2 - V_c}{RI_i} = 0\,, \tag{A-14}$$

$$\exp\left\{\frac{e(\bar{V}_p - \bar{V}_f)}{kT_e}\right\} \exp\left\{-\frac{e(V_m - Ed)}{2kT_e}\right\} - 1 + \frac{\bar{V}_p - V_m/2 - V_c}{RI_i} = 0\,. \tag{A-15}$$

By subtracting eq. (A-14) from eq. (A-15), we obtain the equation

$$\exp\left\{\frac{e(\bar{V}_p - \bar{V}_f)}{kT_e}\right\} = \frac{V_m}{RI_i} \frac{1}{\exp\{e(Ed - V_m)/2kT_e\} - \exp\{-e(Ed - V_m)/2kT_e\}}\,. \tag{A-16}$$

By adding eq. (A-14) to eq. (A-15), we obtain the equation

$$\exp\left\{\frac{e(\bar{V}_p - \bar{V}_f)}{kT_e}\right\}\left[\exp\left\{\frac{e(Ed - V_m)}{2kT_e}\right\} + \exp\left\{-\frac{e(Ed - V_m)}{2kT_e}\right\}\right] - 2 + \frac{2(\bar{V}_p - V_c)}{RI_i} = 0\,. \tag{A-17}$$

By substituting eq. (A-16) in eq. (A-17), we obtain the equation

$$\frac{V_m}{2}\left[\tanh\left\{\frac{e(Ed - V_m)}{2kT_e}\right\}\right]^{-1} - RI_i + \bar{V}_p - V_c = 0\,. \tag{A-18}$$

In the case of no bias, we obtain, for $\bar{V}_p = V_c$, the equation

$$\frac{V_{mo}}{2}\left[\tanh\left\{\frac{e(Ed - V_{mo})}{2kT_e}\right\}\right]^{-1} - RI_i = 0\,, \tag{A-19}$$

where V_{mo} is the output voltage without the bias. From eq. (A-19), we can get the ion current I_i,

$$I_i = \frac{V_{mo}}{2R}\left[\tanh\left\{\frac{e(Ed - V_{mo})}{2kT_e}\right\}\right]^{-1}\,. \tag{A-20}$$

In the case with bias V_B, we obtain for $\bar{V}_p - V_c = -V_B$, the equation

$$\frac{V_{mb}}{2}\left[\tanh\left\{\frac{e(Ed-V_{mb})}{2kT_e}\right\}\right]^{-1} - RI_i - V_B = 0\,, \tag{A-21}$$

where V_{mb} is the output voltage with the bias. By subtracting eq. (A-19) from (A-21), we can get the electron temperature equation

$$\frac{V_{mb}}{\tanh\{e(Ed-V_{mb})/2kT_e\}} - \frac{V_{mo}}{\tanh\{e(Ed-V_{mo})/2kT_e\}} = 2V_B\,. \tag{A-22}$$

If we use an approximation, that is, $\tanh x \simeq x$, we obtain an approximate electron temperature equation as

$$T_e \simeq \frac{eV_B}{k}\left(\frac{1}{Ed/V_{mb}-1} - \frac{1}{Ed/V_{mo}-1}\right)^{-1}. \tag{A-23}$$

No ion current data is needed in order to obtain the electron temperature from eq. (A-23). Figure A-1 shows the relation between the two ratios, V_{mo}/Ed and V_{mb}/Ed, with the electron temperature as a parameter. When the input resistance is too high and the ratio V_{mo}/Ed comes close to unity, it becomes difficult to obtain the electron temperature by this method.

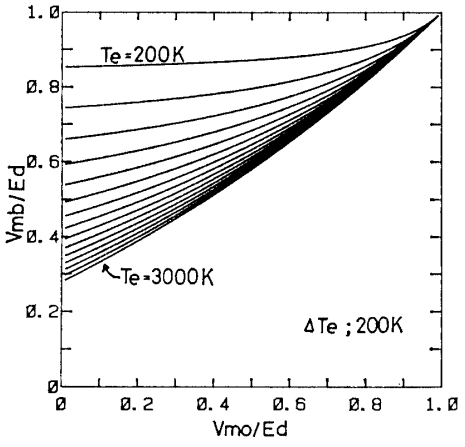

Fig. A-1. A diagram showing relations between V_{mo}/Ed and V_{mb}/Ed with the electron temperature as a parameter.

Next, in order to estimate the electron density N_e, we use the SAGALYN *et al.* (1963) equation for the ion current I_i;

$$I_i = AN_e e\left(\frac{kT_i}{2\pi m_i} + \frac{v_R^2}{16}\right)^{1/2}, \tag{A-24}$$

where A is the effective probe surface area, N_e is the electron density which is assumed to equal the ion density, T_i is the ion temperature, m_i is the ion mass, and v_R is the rocket velocity. We obtain the electron density from eq. (A-20) and eq. (A-24) as

$$N_e = \frac{V_{mo}}{2ARe}\left[\tanh\left\{\frac{e(Ed-V_{mo})}{2kT_e}\right\}\right]^{-1}\left(\frac{kT_i}{2\pi m_i} + \frac{v_R^2}{16}\right)^{-1/2}. \tag{A-25}$$

If we use the approximation, $\tanh x \simeq x$ and the approximate equation (A-23) for the electron temperature, the electron density can be calculated from the equation:

$$N_e \simeq \frac{1}{4\pi r^2} \frac{V_B}{eR_6} \left\{ \frac{V_{mb}(Ed - V_{mo})}{V_{mo}(Ed - V_{mb})} - 1 \right\}^{-1} \left(\frac{kT_i}{2\pi m_i} + \frac{v_R^2}{16} \right)^{-1/2} . \qquad \text{(A-26)}$$

Here, we need the ion temperature, so that we have made the assumption in this paper that $T_e/2 \leqq T_i \leqq T_e$.

Reference

SAGALYN, R. C., SMIDDY, M. and WISNIA, J. (1963): Measurement and interpretation of ion density distributions in the daytime *F* regions. J. Geophys. Res., **68**, 199.